ResearchGate

See discussions, stats, and author profiles for this publication at: https://www.researchgate.net/publication/377599888

Graphite oxide coated sand composites for efficient removal of calcium ions from hard water: isotherm, kinetics, and adsorption mechanism

Article · January 2024

DOI: 10.62753/ctp.2023.05.4.4

CITATIONS
0

READS
144

7 authors, including:

W. P. R. T. Perera
Gampaha Wickramarachchi University of Indigenous Medicine
73 PUBLICATIONS **142** CITATIONS
SEE PROFILE

Samadhi Fernando
Monash University (Australia)
9 PUBLICATIONS **36** CITATIONS
SEE PROFILE

Rajith Akalanka Perera
University of Kelaniya
26 PUBLICATIONS **0** CITATIONS
SEE PROFILE

Janitha A Liyanage
Department of Chemistry, University of Kelaniya, Sri Lanka
173 PUBLICATIONS **440** CITATIONS
SEE PROFILE

All content following this page was uploaded by W. P. R. T. Perera on 23 January 2024.

The user has requested enhancement of the downloaded file.

Polish Society of Composite Materials
Polskie Towarzystwo Materiałów Kompozytowych

23: 4 (2023) 209-219

COMPOSITES THEORY AND PRACTICE
ISSN: 2084-6096
ISSN (online): 2299-128X

W.P.R.T. Perera[1]*, Niroshan Premasinghe[2], W.S.K. Fernando[2], P.L.R.A. Perera[2], Chanaka Sandaruwan[4] A.R. Kumarasinghe[3,5], Janitha A. Liyanage[2]

[1] Gampaha Wickramarachchi University of Indigenous Medicine, Department of Indigenous Medical Resources, Yakkala, Sri Lanka
[2] University of Kelaniya, Department of Chemistry, Kelaniya, Sri Lanka
[3] University of Sri Jayewardenepura, Department of Physics, Nugegoda, Sri Lanka
[4] Sri Lanka Institute of Nanotechnology (SLINTEC), Pitipana, Homagama, Sri Lanka
[5] University of Sri Jayewardenepura, Faculty of Applied Sciences, Center for Nanocomposite Research, Nugegoda, Sri Lanka
**Corresponding author. E-mail: wprtp@gwu.ac.lk*

Received (Otrzymano) 16.07.2023

GRAPHITE OXIDE COATED SAND COMPOSITES FOR EFFICIENT REMOVAL OF CALCIUM IONS FROM HARD WATER: ISOTHERM, KINETICS, AND ADSORPTION MECHANISM

Even if granular media filtration effectively reduces the turbidity of water, its limited surface functionalities and physical properties may constrain its ability to effectively remove critical contaminants from water. In our research, we successfully synthesized a new type of porous material – multiple coated GO/sand (M-GO/S) by integrating ordinary river sand with graphite oxide (GO) for the adsorptive removal of calcium ions in terms of water softening. Prior investigations confirmed it could remove water turbidity and fluoride simultaneously. M-GO/S was characterized using microscopic and spectroscopic techniques. The results indicate the presence of an uneven coating of graphite oxide, and the nanocomposite contains oxygen-containing functional groups. Under given conditions, the M-GO/S nanocomposite demonstrated remarkable efficacy in removing 75% of calcium ions (a higher removal percentage than commercial coal powdered activated carbon) from simulated hard water: pH 8, 5.0 g dosage, 50 mg/L calcium ions, and 20 min contact time. The isotherm and kinetic data revealed that the adsorption mechanism primarily comprises multilayer adsorption by means of a chemical sorption process. The mechanism of the proposed M-GO/S nanocomposite for removing calcium ions from hard water is elucidated using (XPS) analysis. The presence of (-O-Ca-O-) chemical bonds on the surface of the nanocomposite after equilibration with calcium ions suggests the occurrence of chemical interactions between the calcium ions and oxygen-containing functional groups of the M-GO/S. Consequently, the synthesized M-GO/S nanocomposite can be identified as a promising candidate for hard water treatment.

Keywords: graphite oxide, sand, water hardness, adsorption

INTRODUCTION

Access to clean drinking water is crucial for public health owing to the fact that long-term exposure to contaminated water and hard water can lead to chronic health issues [1]. Water hardness can increase the absorption of calcium and magnesium in the body. There is a positive correlation between the magnesium intake from drinking water and a lower risk of hypertension, cardiac arrhythmias, atherosclerosis, and diabetes mellitus. However, an excessive or inadequate intake of calcium may lead to osteoporosis, kidney stones, strokes, and insulin resistance [2]. Hence, the demineralization/softening of water requires innovative methods for calcium ion removal. The pre-treatment stage is crucial [3], and cost-effective approaches require further investigation [4]. Various methods in the recent past have been used to remove water hardness, including electrochemical processes [5], nanofiltration [6], ultra-filtration [7], ion-exchange membranes [8], lime soda softening, and adsorption. Nevertheless, high energy consumption and high operational costs are the limiting factors for full-scale applications of electrochemical processors [9, 10]. Furthermore, adsorption techniques can effectively reduce metal ion concentrations to low levels [11].

Successful adsorption relies on adsorbent properties like the surface area, pore volume, and functionalities [12]. Porous materials (e.g. activated carbon, pillared clays, zeolites, mesoporous oxides, polymers, and metal-organic frameworks) remove pollutants from the air, water, and soil [13, 14]. Graphite oxide (GO) has gained significant attention in the scientific community in recent years due to its exceptional stability, abundant functional groups, and large specific surface area [15]. Nonetheless, as it easily disperses in water, this makes it challenging to be reused in adsorption processes. Therefore, developing composites incorporating sand and graphite oxide (GO) can circumvent the limitations of using GO alone [16]. Sand has been widely em-

ployed in water treatment processes for mitigating turbidity [17, 18], while GO has shown promising capabilities in effectively removing water contaminants. By combining sand and GO, the resulting composites can potentially synergize their unique advantages, providing a good approach for water treatment applications [19, 20].

A coating with GO can improve the normal filter performance of sand in water treatment units [18]. The method involves creating a composite material with a core-shell structure, where the sand granules serve as the core and water-dispersible graphite oxide nanosheets are assembled onto the sand surface as the shell [21-24]. Meanwhile, researchers have also investigated different GO/sand composites for ion adsorption tasks. For example, a GO/sand composite synthesized from sugar and sand was successfully employed as an effective and economically viable adsorbent in removing Cr (VI) from water [25]. Polymer-based GO nanocomposites, such as epoxy resin nanocomposites [26], have been found to improve the mechanical strength of composites. Moreover, surface-modified GO/sand composites have been studied for different adsorption approaches. For instance, its surface properties have made it suitable for investigating the ion absorption capacities of various divalent metals Cd(II), Cu(II), Pb(II), and Zn(II), thereby creating a novel approach for the mitigation of metals from water [27]. Additionally, previous studies have examined the adsorption capability of GO for various metal ions, including Co(II), Cd(II), U(VI), and Eu(III). The adsorption capacities were reported as 106.3, 68.2, 175.4, and 97.5 mg g^{-1}, respectively [28, 29]. Furthermore, Thompson et al. investigated the adsorption competencies of divalent metal ions (Hg(II), Cd(II), Zn(II), and Cu(II)) by GO via computational investigations: density functional theory. Accordingly, the research study found that metal ions bind more efficiently to the surface of graphite oxide (GO) in the following order: $Cu2^{+} > Hg^{2+} > Zn^{2+} > Cd^{2+}$ [30]. In addition to the utilization of graphite oxide (GO) and its composites, activated carbon (AC) is the preferred sorbent for the adsorption of metal ions from polluted water. A recent study that examined the adsorption of water hardness using AC demonstrated that the synthesized AC possessed an adsorption capacity of 69.6% in optimal conditions [31].

Our previous studies proved that a five-time coated GO/sand nanocomposite regulates excess fluoride ions and turbidity in water simultaneously (over 70% fluoride removed around pH 7.00 ± 0.02 and 87% turbidity reduced at the same time) [32]. Apart from that, the management of excessive calcium levels in water is essential as it can cause detrimental health effects on humans and lead to destructive conditions in water sources. Hence, our current study aims to explore the adsorption potential of calcium ions by graphite oxide nanosheet coated sand, elucidating the underlying adsorption mechanism to assess the feasibility of employing the M-GO/S nanocomposite for practical applications in large-scale production.

EXPERIMENTAL

Materials

The natural vein graphite (NVG) utilized in this study was sourced from the Bogola mines in Sri Lanka (located at 7°06'58.49"N, 80°18'34.41"E). The purity of the graphite was determined by ash content analysis and was greater than 99%. The sand sample used in the study was procured from the Mahaweli River (8°27'59.99"N, 81°13'60.00"E) in Sri Lanka. Coal powdered activated carbon (200 US Mesh pore size) was purchased. The experiments were conducted using chemicals of analytical grade, which were obtained from Sigma-Aldrich (USA), BDH (UK), or Fluke (Switzerland). Throughout the study, ultrapure water was employed.

Synthesis of M-GO/S nanocomposite

The synthesis of graphite oxide (GO) was performed using the improved Hummers method (IHM) [33], utilizing natural vein graphite (NVG) as the starting material. The NVG was obtained from Bogola mines in Sri Lanka and was found to have a purity of better than 99.95%, as determined by ash content analysis (ASTM D 6349-09) [34]. The graphite oxide slurry produced from the chemical oxidation of NVG was thoroughly washed with ultrapure water till the pH of the solution became neutral. A small volume of the pH-neutral graphite oxide suspension was thinned down using distilled water (approx. 1 mg/mL) and subjected to ultrasound treatment (150 W, Grant, UK) for 20 min. The resulting GO dispersion was maintained by stirring (at 120 rpm) at ambient temperature for 12 h.

River sand, commonly employed in water filtration processes, was characterized by its chemical composition consisting predominantly of SiO_2 (95%) with minor amounts of Fe_2O_3 (2.00%), Al_2O_3 (1.11%), CaO (1.72%), MgO (0.10%), and negligible loss on ignition (0.05%). The particle size of the river sand varied between 0.425 and 0.600 mm, with an estimated average surface area of 70 cm^2/g. To eliminate surface impurities, the sand underwent a series of purification treatments, including washing with 0.1 mol/L HNO_3, rinsing with distilled and deionized water, soaking in 0.1 mol/L NaOH for three hours, and additional rinsing with distilled water. The purification process was concluded by drying the sand at 110°C for two hours. GO/sand composites were synthesized according to the procedures given by A.R. Kumarasinghe et al. [32]. Hereafter, unless otherwise stated, we use the following notations for the GO/sand nanocomposites: S-GO/S – GO coating in one cycle; M-GO/S – GO coating in multiple cycles (Fig. 1).

 All rights reserved

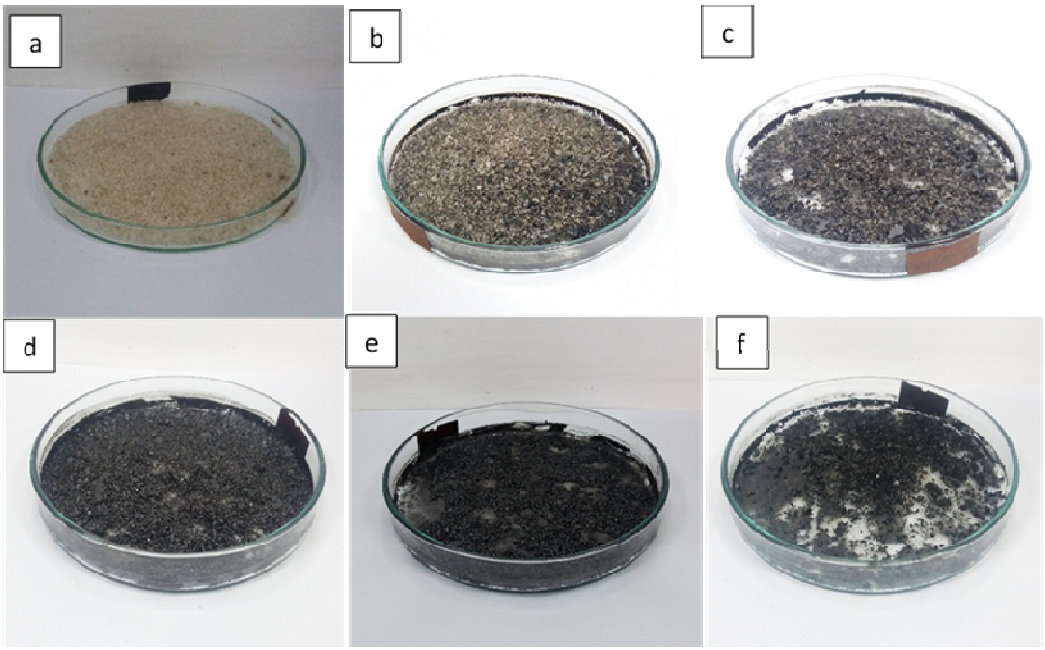

Fig. 1. Purified sand (a), single coated GO/sand nanocomposite (S-GO/S) (b), two-time coated GO/sand nanocomposite (2-M-GO/S) (c), (3-M-GO/S) (d), (4-M-GO/S) (e), (5-M-GO/S) (f)

Optimization studies for calcium ion absorption by GO/sand composites

To select an efficient GO/sand nanocomposite for the adsorption of calcium from the water, a 50 mg/L calcium ion solution was equilibrated with S-GO/S, M-GO/S, and normal purified river sand. 200 US Mesh coal powdered activated carbon was used as the control adsorption material to compare the calcium mitigation capabilities with the synthesized GO/sand composite. The adsorption capacity of the calcium by the coal powdered activated carbon was reported as 64% in the given conditions (initial calcium concentration 50 mg/L, dosage 5 g, 1 hour contact time at neutral pH). The calcium ion removal percentages were calculated, and the highest ion removal efficiency was obtained by M-GO/S (75%) (Fig. 2).

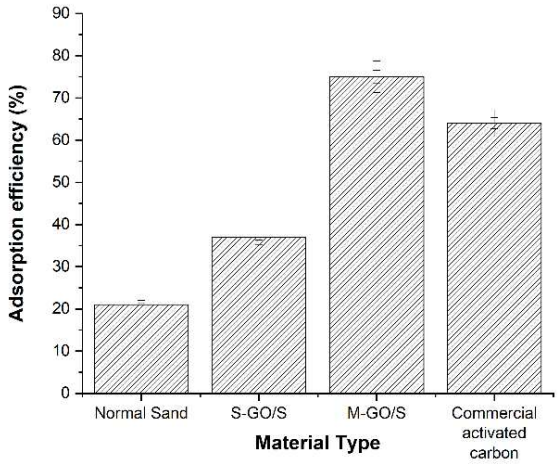

Fig. 2. Calcium mitigation efficiencies by normal sand, S-GO/S, and M-GO/S and -activated carbon (initial calcium concentration 50 mg/L, dosage 5 g, 1 hour contact time at neutral pH – error bars in ± SD)

Batch trials were conducted to determine the optimal conditions for calcium ion adsorption by M-GO/S. Various factors such as the pH value, equilibration time, solid nanocomposite content, and initial calcium ion concentration were investigated to identify the most suitable conditions.

Characterization of GO/sand composite

The morphology of the single and multiple coated GO/sand composites was examined using a scanning electron microscope (Zeiss Quanta 650 FEG) and the elemental composition of the surface of the M-GO/S before and after the adsorption of calcium was recorded by energy dispersive X-ray spectroscopy (EDX) in SEM. X-ray diffraction (XRD) analysis (Rigaku D-max 2500 instrument (Japan), using Cu Ka radiation, voltage of 40 kV and current of 30 mA) was conducted to determine the crystalline structure of the acquired river sand and to evaluate the conversion of graphite to graphite oxide. To validate the adsorption of calcium ions on M-GO/S and gain insights into the underlying adsorption mechanism, X-ray photoelectron spectroscopy (XPS) (Thermo Scientific ESCALAB Xi+) was utilized to investigate the surface composition of M-GO/S before and after the adsorption of calcium ions.

Isotherm studies and kinetic modeling

The adsorption isotherm experiments were conducted in 100 mL Erlenmeyer flasks containing 25 mL of M-GO/S (5.0 g) and initial calcium concentrations of 10-60 mg/L, fixed at pH 8. The solutions were agitated at 60 rpm at room temperature (28°C) for 20 minutes. Filtrates of the liquid phases were passed through membrane filters (0.45 μm), and the residual calcium

 All rights reserved

ions in the filtrates were quantified by ICP-MS analysis.

A batch-mode experiment assessed the kinetics of calcium ion adsorption by M-GO/S. A 500 mL water-jacketed batch reactor was utilized, containing a 50.0 mg/L calcium solution and 5 g of M-GO/S under a continuous flow of N_2. The solution was agitated at 60 rpm and maintained at the temperature of 28°C for 20 minutes. Aliquots (10 mL) were sampled at predetermined time intervals (every 2 minutes), the filtrates of the liquid phases were passed through the filters (0.45 μm), and the residual calcium ions in the filtrates were quantified by ICP-MS analysis. The pH of the solution was kept at 8. The number of absorbed calcium ions and the adsorbed percentage was calculated using the following established equations:

$$Adsorbed\ amount\ \left(\frac{mg}{g}\right) = \frac{C_i - C_f}{m} V \quad (1)$$

$$Adsorbed\ percentage\ = \frac{C_i - C_f}{C_i} \times 100 \quad (2)$$

where C_i is the initial concentration, C_f is the final concentration of calcium ion solution [mg/L], V is the volume of the adsorbate solution, and m is the weight of the adsorbent.

RESULTS AND DISCUSSION

Surface morphology of GO/sand composites

Figure 3 shows plain view SEM micrographs of S-GO/S. The micrographs were acquired in the secondary electron imaging (SEI) mode. The SEM micrographs showed wrinkled surface morphology for GO and the GO/sand nanocomposite as irregularly shaped granules. Nevertheless, it was observed that the GO coating on the sand surface was not spread continuously. Following the application of the fifth coating of GO on the sand surface, a gradual reduction of uncoated sand particle regions and a progressive increment in the thickness of the GO layer were observed. Furthermore, the rough surface observed in the uncoated areas becomes smoother, indicating the deposition of GO layers on it.

SPECTROSCOPIC CHARACTERIZATION

Energy dispersive X-ray spectroscopy (EDX)

The EDX spectrum was recorded and compared between M-GO/S before and after the adsorption of calcium (Fig. 4) for elemental analysis. The spectrum of M-GO/S shows peaks for C (45.64%), O (36.19%), and Si (18.17%). The conspicuous peak obtained for C appears from graphite's basal plane of carbon atoms, and the Si peak may be due to uneven GO coating on the sand grains. The O peak is generated on the spectrum due to the graphite surface functionalized with the oxygen-containing groups (Fig. 4a). The EDX spectrum after absorption of the calcium ions on M-GO/S is shown in Figure 4b, depicting similar C, O, and Si percentages to Figure 4a. In addition to the C, O, and Si peaks, a small peak for Ca appears in Figure 5b (Ca-0.31%), proving that calcium ions adhered to the surface of M-GO/S.

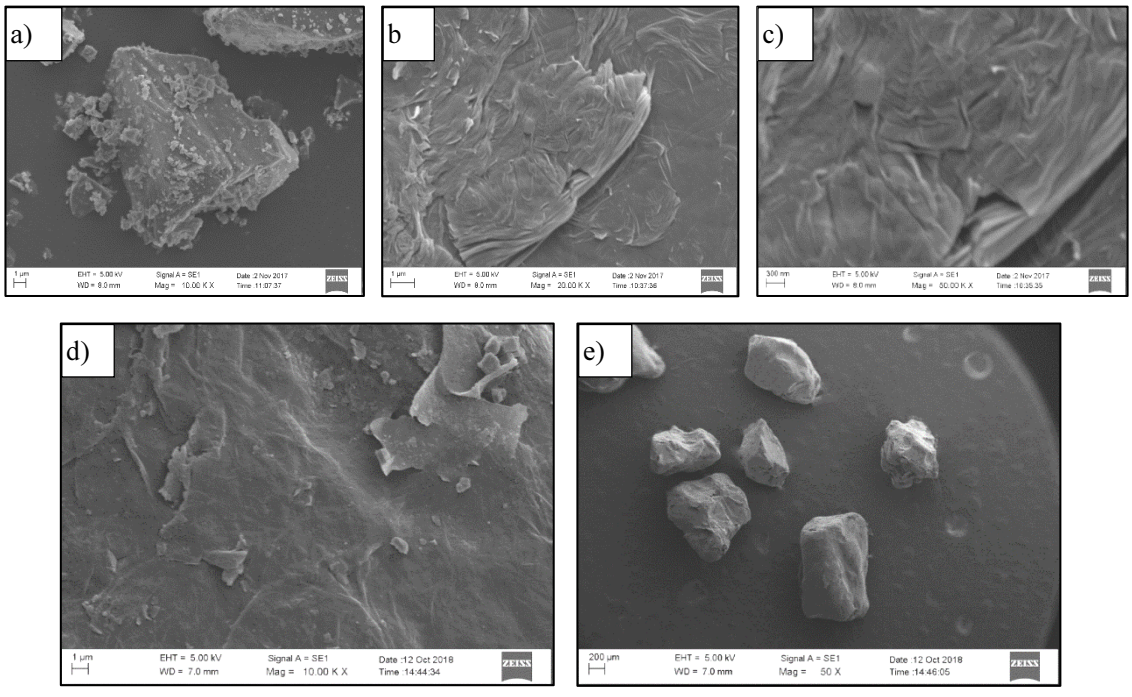

Fig. 3. SEM micrographs of S-GO/S under three magnifications: a) 10.00 KX, b) 20.00 KX, c) 50.00 KX and SEM micrographs of M-GO/S under two magnifications: d) 10.00 KX, e) 50 X

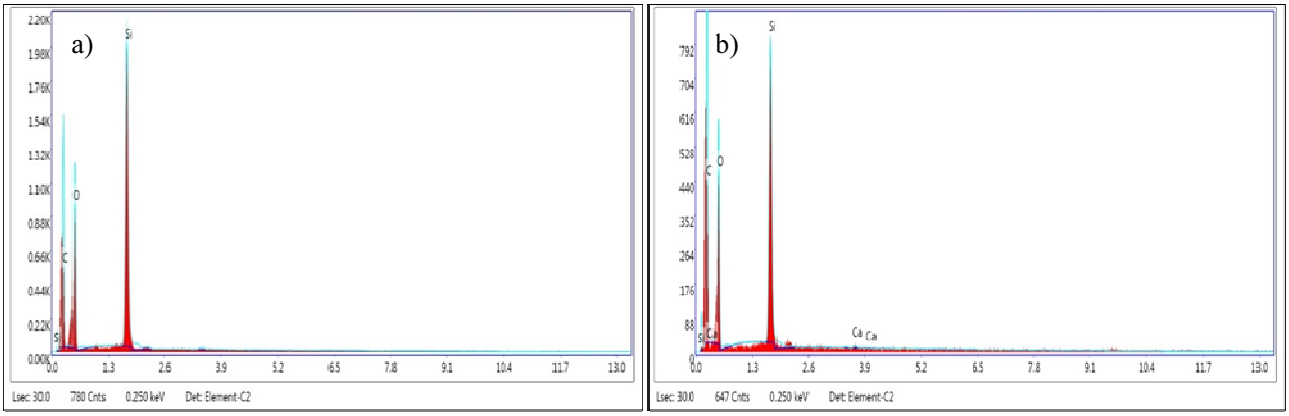

Fig. 4. EDX spectrum of: a) M-GO/S and b) M-GO/S after adsorption of calcium

X-ray diffraction (XRD) spectral analysis

To identify the crystalline structure of the procured river sand and to assess the transformation of graphite-to-graphite oxide, X-ray diffraction (XRD) analysis was performed in a laboratory setting (Fig. 5). The (0 1 1) plane exists at 26.60° for quartz as the primary crystalline material of the river sand [35]. The XRD spectra of graphite and GO were also obtained and are shown in Figure 5. The XRD pattern of GO synthesized using the modified Hummers method revealed the presence of the (0 0 1) crystal plane, displaying an interlayer spacing of 8.396 Å, a characteristic feature of GO [36]. Furthermore, the X-ray diffraction (XRD) peaks corresponding to the (0 1 1) crystal plane of sand and the (0 0 2) crystal plane of graphite are in close proximity and exhibit a significant overlap, making them difficult to distinguish from one another. Thus, the validity of the graphite oxide synthesis procedure employed in this study was confirmed through the detection of the characteristic 2θ peak at 10.04°, indicative of graphite oxide, and the absence of the 2θ peak at 26.10° typically present in graphite.

The observed interlayer spacing for natural vain graphite was 3.36 Å. The increase in GO spacing was due to the incorporation of functional groups at the edges and between the layers. In the XRD spectrum of M-GO/S, the typical GO peak around 8.396 Å disappeared, presumably due to the disordered GO layers on the surface of the sand during coating. Owing to the repetition of the heating procedure when synthesizing M-GO/S, GO may embed on the surface of the sand in a thoroughly exfoliated manner due to the reduction in interlayers resulting in a new exfoliated structure without a specific XRD signature for M-GO/S.

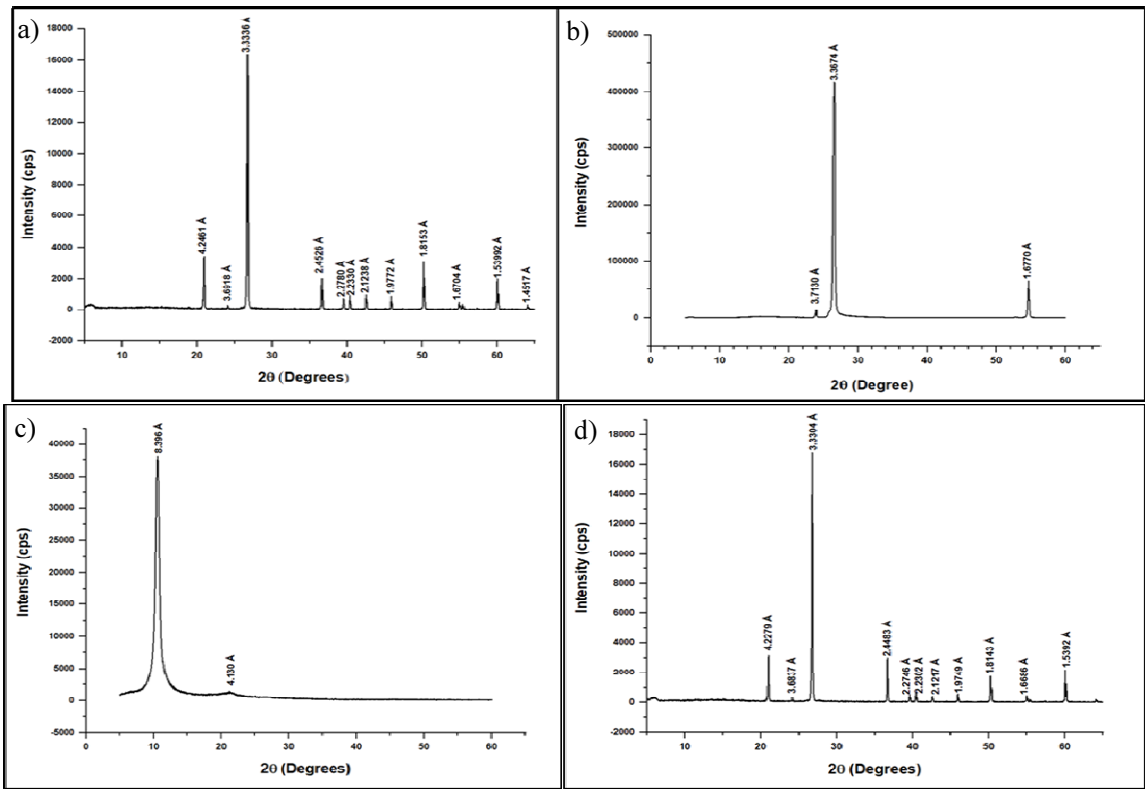

Fig. 5. XRD spectrum of: a) purified sand, b) graphite, c) graphite oxide, d) M-GO/S with Cu Ka radiation, voltage of 40 kV and current of 30 mA

X-ray photoelectron spectroscopy (XPS)

To authenticate the adsorption of calcium ions on M-GO/S and to understand the underlying adsorption mechanism, XPS was employed to examine the surface composition of M-GO/S before and after Ca ion adsorption. The XPS analysis results indicated the presence of a Ca (2p) peak in the M-GO/S spectrum after adsorption, signifying the occurrence of chemical bonding between the M-GO/S surface and Ca Ions (Fig. 6a and b).

A comprehensive analysis of the Carbon 1s (C 1s) spectra of the M-GO/S sample before calcium ion adsorption revealed the existence of four distinct carbon species exhibiting binding energies at 284.8 eV, 287.05 eV, and 288.85 eV. These carbon species were identified as the C-C/C-H, C-O, and COO (epoxy) functional groups, respectively, as shown in Figure 6c [37]. Further XPS analysis of the M-GO/S sample post-calcium ion adsorption revealed a similar peak pattern to the pre-adsorption spectrum, albeit with diminished peak intensities and altered positions of the peaks. These findings provide substantiation for the notion that the oxygen-containing functional groups that are present on the surface of graphite oxide (GO) are involved in the adsorption of metal ions via chemical interactions [32] (Fig. 6d).

The de-convoluted O 1s spectrum of the M-GO/S before the absorption of calcium ions showed a peak centered at the binding energy of 532.97 eV (Fig. 6e) [38, 39], which can be assigned to the C-O bonding of oxygen. Nevertheless, the O 1s spectrum of the M-GO/S after Ca ion absorption exhibited two distinct peaks centered at binding energies of 532.76 eV and 531.27 eV. The former peak can be attributed to C-O bonding, while the latter, a smaller peak, can be feasible to assign Ca-O bonding [40] as depicted in Figure 6f.

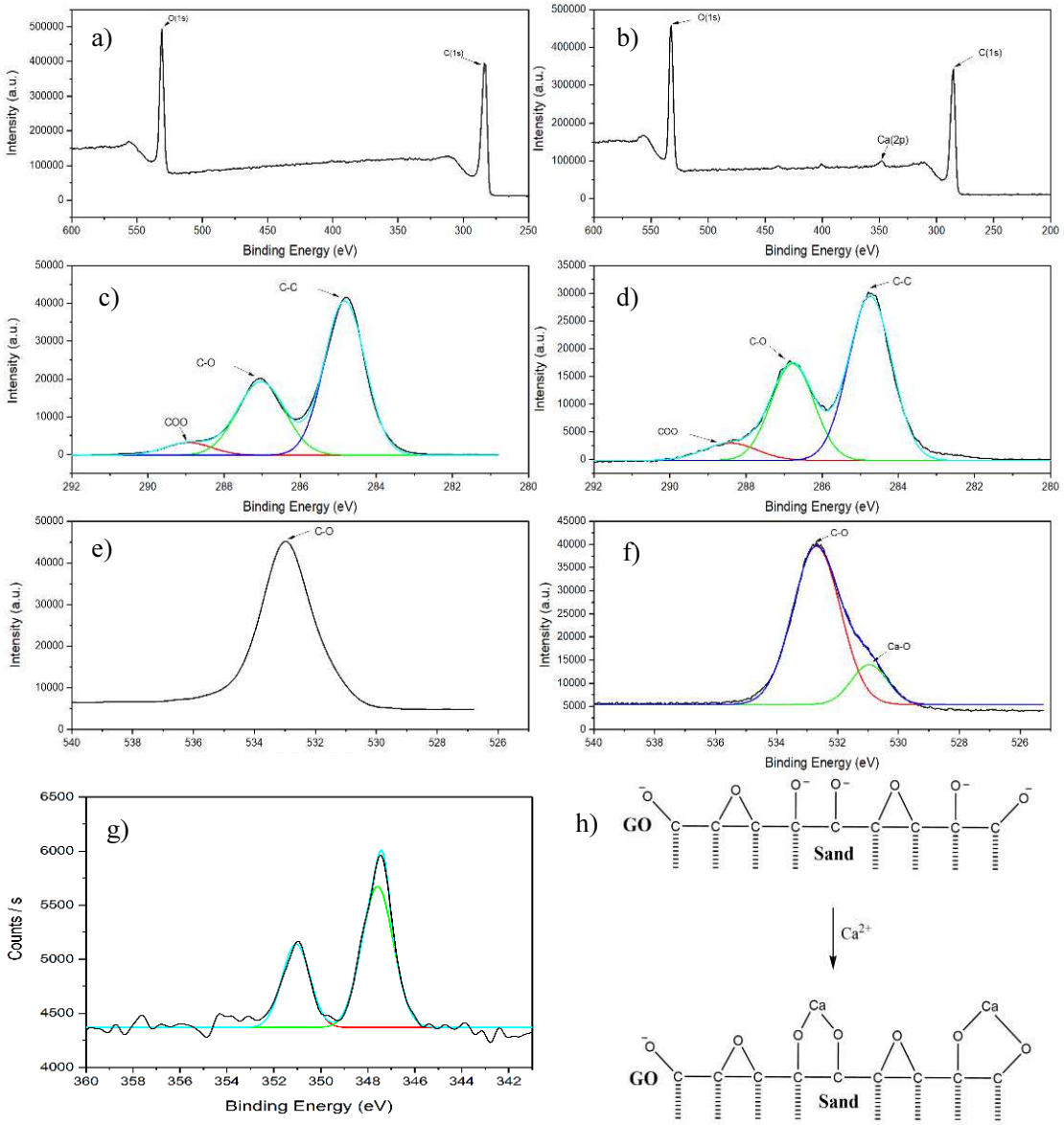

Fig. 6. XPS spectrum (survey) of: a) M-GO/S before adsorption of calcium and b) M-GO/S survey spectrum after adsorption of calcium, c) detailed analysis of Carbon 1s (C 1s) spectra of M-GO/S sample before calcium ion adsorption and d) after adsorption, e) de-convoluted O (1s) spectrum of M-GO/S before absorption of calcium ions and f) after adsorption of calcium ions, g) de-convoluted Ca (2p) spectrum of M-GO/S after adsorption of calcium ions, h) proposed mechanism for chemisorption of calcium ions on M-GO/S

 All rights reserved

Furthermore, the de-convoluted Ca(2p) peak was split into two distinct peaks (Fig. 6(g)), and it may be a consequence of spin-orbit coupling, which causes the energy levels of the 2p1/2 and 2p3/2 states to split. Furthermore, these states arise owing to the coupling between the electron's spin and its orbital angular momentum. The spin-orbit coupling causes the energy levels of the 2p1/2 and 2p3/2 states to split, resulting in two peaks in the XPS spectrum [41]. Our findings suggest that the equilibration of calcium ions with the M-GO/S nanocomposite results in chemical bonds between oxygen and calcium (O-Ca-O), as evidenced by the XPS spectroscopic analysis (Fig. 6h).

Meanwhile, a detailed FT-IR analysis was also conducted on M-GO/S [32], confirming the presence of various functional groups, including C=O, O=C-OH, C-O, C-O-C, and Si-O, on the surface of the nanocomposite. These findings highlight the successful integration of the properties of graphite oxide and sand synergistically onto the surface of M-GO/S.

OPTIMIZATION STUDIES

The pH of the solution considerably influences the adsorption behavior of calcium ions. In this study, the adsorption efficiency of calcium ions was evaluated across a pH range of 3-11, revealing that the highest adsorption occurred at pH 8, as seen in Figure 7a. However, the adsorption percentage fluctuated at different pH values, suggesting that the adsorption mechanism may not be solely governed by physisorption but also involves a significant contribution from chemisorption [42]. The most effective calcium ion concentration was 50 mg L^{-1} (Fig. 7b). Apart from that, when increasing the adsorbate dosage, the calcium ion removal percentage increased until the dosage equaled 5.0 g and then decreased (Fig. 7c). An increase in the quantity of adsorbent led to a corresponding rise in the availability of adsorption sites. Nevertheless, as the material's steric hindrance reached a certain point, further additions of adsorbent did not significantly enhance the removal efficiency [43].

The temporal correlation between the contact time and calcium ion adsorption on the surface of M-GO/S revealed an equilibrium after 20 minutes (Fig. 7d) with subsequent stabilization of the adsorption rate. The initial rise in the adsorption rate can be attributed to the availability of vacant adsorption sites. Nonetheless, a prolonged contact time may reduce adsorption because of repulsive interactions between the adsorbed metal ions and solution ions, impeding further adsorption [44].

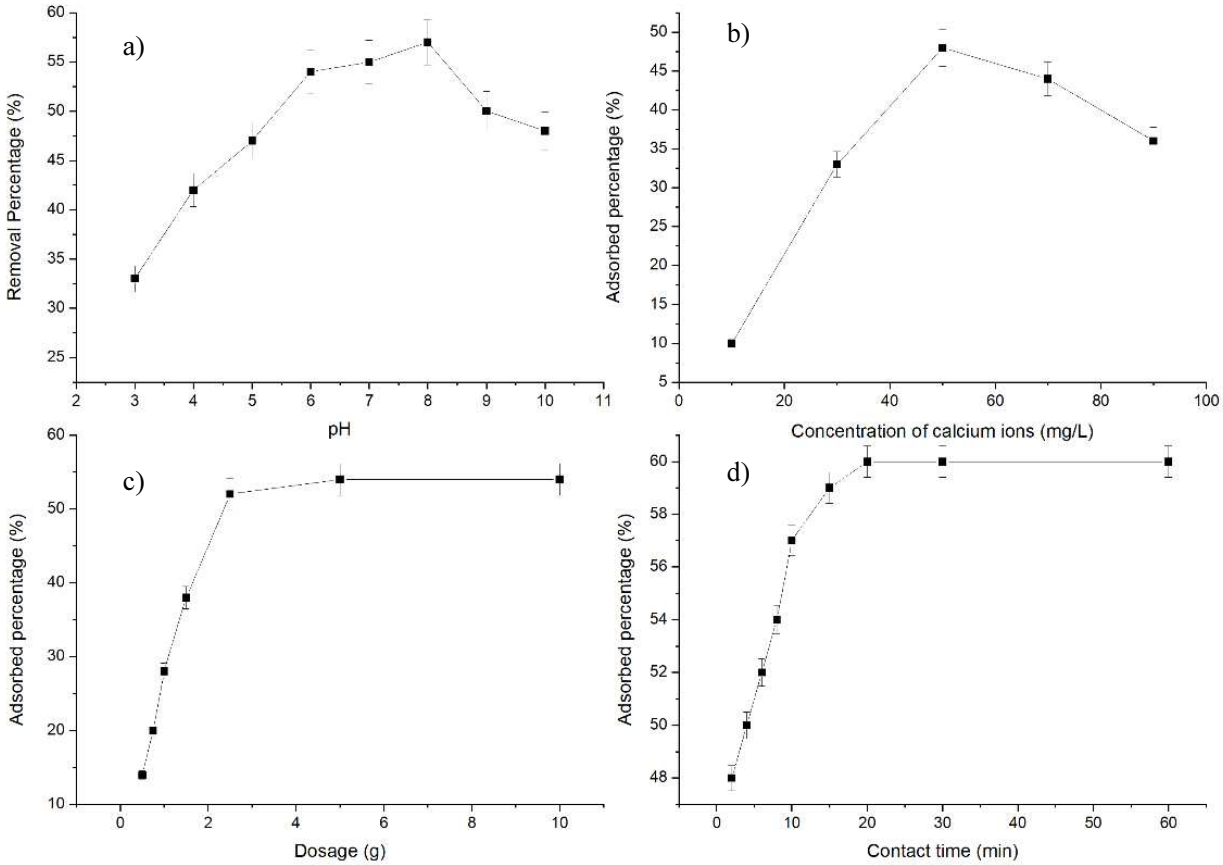

Fig. 7. Optimization studies of calcium ion adsorption/removal by M-GO/S: a) pH (at 50 mg/L of calcium, 5.0 g dosage, and 1 h contact time), b) initial calcium ion concentration (at pH 8, 5.0 g dosage, and 1 h contact time), c) dosage of granules (at pH 8, 50 mg/L of calcium, and 1 h contact time), d) contact time (at pH 8, 50 mg/L of calcium, and 5.0 g dosage)

 All rights reserved

Calcium absorption isotherm

The Langmuir isotherm model presented by Irving Langmuir [45] describes the theoretical concept that only a single-layer adsorption process happens on an adsorbent and assumes that all active sites are uniform and independent of each other [46, 47].

The linearized form of the Langmuir equation can be expressed as [48, 49]

$$\frac{C_e}{q_e} = \frac{1}{K_L . Q_{max}} + \frac{C_e}{Q_{max}} \tag{3}$$

where: q_e – equilibrium adsorption capacity [mg/g], Q_{max} – maximum adsorption capacity [mg/g], C_e – equilibrium concentration of adsorbate [mg/L], K_L – constant related to the energy of adsorption [L/mg]. Thus, plotting C_e/q_e against C_e yields a slope of $1/Q_{max}$ and an intercept of $1/K_L Q_{max}$.

According to the Freundlich isotherm model, a multilayer adsorption process can be assumed [33]. The linear pattern of the Freundlich equation can be represented as [50]

$$logq_e = logQ_F + \frac{1}{n} logC_e \tag{4}$$

where: Q_F and n are the Freundlich constants, Q_F – capacity, n – intensity, C_e – equilibrium concentration in solution, Q_e – adsorbed capacity.

To determine the most appropriate model for the desired adsorption process, the correlation coefficient value (R^2) was assessed. The R^2 values for the Langmuir and Freundlich adsorption isotherms were 0.8936 and 0.9871, respectively. Based on the results, the Freundlich adsorption isotherm model was appropriate for the adsorption of calcium ions on M-GO/S, as the corresponding R^2 value was 0.9871. Consequently, it can be deduced that the adsorption mechanism operates through multilayer adsorption. Furthermore, parameter n in the Freundlich isotherm reflects the nonlinearity between adsorption and the solution concentration: $n = 1$ indicates a linear relationship, $n < 1$ indicates a chemical adsorption process, and $n > 1$ indicates physical adsorption [51, 52]. The n value for the isotherm studies was observed as 0.0201 (Table 1), demonstrating a chemical adsorption process between the calcium ions and the surface of M-GO/S.

Kinetic model

One commonly used equation for the adsorption of adsorbate from an aqueous solution is Lagergren's kinetics equation [53]. The following equation, which corresponds to pseudo-first-order, can be written as [54]:

$$\log(q_e - q_t) = logq_e - \frac{K_{1,ads} t}{2.303} \tag{5}$$

where: q_t – the number of calcium ions adsorbed per mass of sorbent [mg/g] at any time; q_e – the number of calcium ions adsorbed per mass of sorbent [mg/g] at equilibrium, $K_{1,ads}$ – the rate constant of first-order adsorption [min^{-1}]. The straight-line plot of log ($q_e - q_t$) vs. t gives the log (q_e) slope and intercept equal to $K_{1,ads}/2.303$.

The equations for the pseudo-second-order kinetics can be written as [54]:

$$\frac{t}{q_t} = \frac{1}{K_{2,ads} q_e^2} + \frac{t}{q_e} \tag{6}$$

where: q_t – quantity of calcium ions absorbed per unit mass of sorbent [mg/g] at any given time, q_e – number of calcium ions adsorbed per unit mass of sorbent [mg/g] at equilibrium, $K_{2,ads}$ – the rate constant of second-order adsorption [g (mg min)$^{-1}$]. The plot of t/q_t vs. t gives $1/q_e$ as the slope and $1/(K_{2,ads}\, q_e^2)$ as the intercept.

Based on the kinetic parameters calculated and presented in Table 1, the correlation coefficients obtained from the pseudo-first-order model (PSO) for calcium ion adsorption on M-GO/S were found to be inadequate (less than 0.8), indicating a weak association between the data and the model. However, the pseudo-second-order model exhibited a correlation coefficient of 1, indicating excellent agreement between the model and the data. These findings suggest that the process involves chemical adsorption on M-GO/S [55].

TABLE 1. **Isotherm and kinetic parameters for adsorption of calcium ions on M-GO/S**

Langmuir constants				Freundlich constants		
Q_{max} [mg/g]	K_L [L/mg]	R_L	R^2	Q_F	n	R^2
0.7587	0.021	0.4878	0.8936	1.2458	0.0201	0.9871
Pseudo-first-order kinetic model				Pseudo-second-order kinetic model		
$K_{1,ads}$ [min^{-1}]	q_e [mg/g]	R^2		$K_{2,ads}$ [g (mg min)$^{-1}$]	q_e [mg/g]	R^2
5.7575×10^{-3}	1.074	0.7812		18.277	0.271	1

The Freundlich and PSO models can be complementary in a dynamic adsorption system. While the PSO model is well-suited to describe the rate of adsorption better, the Freundlich isotherm provides insight into the intensity and capacity of the adsorption at equilibrium [56]. The adsorption sites on graphite oxide (GO) exhibit non-uniform distribution, making the Freundlich isotherm suitable owing to its consideration of a heterogeneous surface. According to the PSO model, a chemisorption process is indicated, highlighting the initial adsorption of calcium ions onto accessible, high-energy sites on GO. These sites promote robust chemical bonding between GO and calcium ions, suggesting a monolayer coverage [57]. As these sites become saturated over time and the adsorption process continues, weaker physisorption can occur, contributing to multilayer adsorption. This is where the Freundlich isotherm

 All rights reserved

becomes relevant as it accommodates the possibility of adsorbate-adsorbate interactions. The employment of both models implies that the system is likely to undergo progression from an initial chemisorption phase (monolayer) to a subsequent phase where the significance of multilayer physisorption increases. This transition between states is not strictly discrete [58].

Strategic coating of graphite oxide on sand surface

The incorporation of sand in conjunction with graphite oxide (GO) in our synthesized composite is motivated by strategic considerations as the standalone utility of GO is hindered by practical challenges. The synthesis of M-GO/S offers various benefits beyond the utilization of GO alone, such as a greater surface area and the prevention of aggregation [59]. The presence of sand provides a structured matrix for GO that is not only easier to handle but also more robust, facilitating practical application and post-treatment recovery [60]. Sand provides significant weight and settling capabilities to the composite, allowing relatively straightforward separation from treated water. Apart from that, as an unmodified adsorbent, sand possesses a relatively low adsorption capacity and specificity for metal ions when compared to engineered adsorbents. In water treatment systems, sand can be prone to fouling by organic and biological matter, which may diminish its adsorption capacity over time and necessitate further treatment or replacement [61]. Through the integration of the surface characteristics of both sand and graphite oxide (GO), the composite material is designed to maximize its ability to adsorb both positive and negative ions. This approach aims to overcome the limitations associated with using sand and GO as standalone adsorbents [32].

CONCLUSIONS

Innovative materials are needed to tackle the hardness caused by calcium and magnesium ions in water sources. This problem is widespread in potable and marine water, and addressing it is crucial due to its impact on water quality and salinity in aquatic environments. Our research has successfully developed an adsorbent with a graphite oxide (GO)/sand core-shell structure (M-GO/S) that effectively removes calcium ions from water. Upon the equilibration of calcium ions with the M-GO/S nanocomposite, the formation of chemical bonds between the oxygen of functional groups and calcium (O-Ca-O) was observed and proposed as the underlying mechanism of calcium ion adsorption. This absorbent also demonstrated the simultaneous removal of fluoride ions and reduction in water turbidity, showcasing its multifunctional capabilities in previous studies. The results obtained from this study hold immense importance concerning the simultaneous effective elimination of water contaminants to achieve optimal water purification efficiency. Further research is warranted to optimize the adsorption efficiency of the M-GO/S absorbent for other cations in water. Additionally, a comprehensive evaluation of the reusability of M-GO/S is essential to establish its sustainability as a viable solution in water treatment applications.

Acknowledgments

Funding for this project was obtained from the research project PS/DSP/ CKDU/06/3.5 entitled "Establish a CKDu Information and Research Center at the University of Kelaniya, Sri Lanka". The authors thank Amila T. Kannangara, Amitha Suriyaarachchi, Erandi Udayasiri, and Sudesh Hemal for their valuable assistance in the sample analysis.

REFERENCES

[1] Hasan M.K., Shahriar A., Jim K.U., Water pollution in Bangladesh and its impact on public health, Heliyon 2019, August, 1, 5(8), DOI: 10.1016/j.heliyon.2019.e02145.

[2] Kozisek F., Regulations for calcium, magnesium, or hardness in drinking water in the European Union member states, Regulatory Toxicology and Pharmacology 2020, April, 1, 112, 104589. DOI: 10.1016/j.yrtph.2020.104589.

[3] Zhao X., Song L., Fu J., Tang P., Liu F., Adsorption characteristics of Ni (II) onto MA–DTPA/PVDF chelating membrane, Journal of Hazardous Materials 2011, May, 30, 189(3), 73240 40, DOI: 10.1016/j.jhazmat.2011.03.061.

[4] Zeppenfeld K., Electrochemical removal of calcium and magnesium ions from aqueous solutions, Desalination 2011, August, 15, 277(1-3), 99-105, DOI: 10.1016/j.desal. 2011.04.005.

[5] Amarasooriya A.A., Kawakami T., Removal of fluoride, hardness and alkalinity from groundwater by electrolysis, Groundwater for Sustainable Development 2019, October, 1, 9, 100231, DOI: 10.1016/j.gsd.2019.100231.

[6] Wang Y., Ju L., Xu F., Tian L., Jia R., Song W., Li Y., Liu B., Effect of a nanofiltration combined process on the treatment of high-hardness and micropolluted water, Environmental Research 2020, March, 1, 182, 109063, DOI: 10.1016/j.envres.2019.109063.

[7] Garba M.D., Usman M., Mazumder M.A., Al-Ahmed A., Inamuddin, Complexing agents for metal removal using ultrafiltration membranes: a review, Environmental Chemistry Letters 2019, September, 1, 17, 1195-208, DOI: 10.1007/s10311-019-00861-5.

[8] Hansima M.A., Makehelwala M., Jinadasa K.B., Wei Y., Nanayakkara K.G., Herath A.C., Weerasooriya R., Fouling of ion exchange membranes used in the electrodialysis reversal advanced water treatment: A review, Chemosphere 2021, January, 1, 263, 127951, DOI: 10.1016/j. chemosphere.2020.127951.

[9] Li Z., Wang R., Young R.J., Deng L., Yang F., Hao L., Jiao W., Liu W., Control of the functionality of graphene oxide for its application in epoxy nanocomposites, Polymer 2013, November, 1, 54(23), 6437-6446, DOI: 10.1016/j.polymer. 2013.09.054.

[10] Sitko R., Turek E., Zawisza B., Malicka E., Talik E., Heimann J., Gagor A., Feist B., Wrzalik R., Adsorption of divalent metal ions from aqueous solutions using graphene oxide, Dalton Transactions 2013, 42(16), 5682-5689, DOI: 10.1039/C3DT33097D.

 All rights reserved

[11] Carolin C.F., Kumar P.S., Saravanan A., Joshiba G.J., Naushad M., Efficient techniques for the removal of toxic heavy metals from the aquatic environment: A review, Journal of Environmental Chemical Engineering 2017, June, 1, 5(3), 2782-2799, DOI: 10.1016/j.jece.2017.05.029.

[12] Wang S., Sun H., Ang H.M., Tadé M.O., Adsorptive remediation of environmental pollutants using novel graphene-based nanomaterials, Chemical Engineering Journal 2013, June, 15, 226, 336-347, DOI: 10.1016/j.cej.2013.04.070.

[13] Wang S., Peng Y., Natural zeolites as effective adsorbents in water and wastewater treatment, Chemical Engineering Journal 2010, January, 1, 156(1), 11-24, DOI: 10.1016/j.cej.2009.10.029.

[14] Ngah W.W., Teong L.C., Hanafiah M.M., Adsorption of dyes and heavy metal ions by chitosan composites: A review, Carbohydrate Polymers 2011, February, 1, 83(4), 1446-1456, DOI: 10.1016/j.carbpol.2010.11.004.

[15] Gong J.L., Zhang Y.L., Jiang Y., Zeng G.M., Cui Z..H, Liu K., Deng C.H., Niu Q.Y., Deng J.H., Huan S.Y., Continuous adsorption of Pb(II) and methylene blue by engineered graphite oxide coated sand in fixed-bed column, Applied Surface Science 2015, March, 1, 330, 148-157, DOI: 10.1016/j.apsusc.2014.11.068.

[16] Luo X., Wang C., Luo S., Dong R., Tu X., Zeng G., Adsorption of As(III) and As(V) from water using magnetite Fe_3O_4-reduced graphite oxide-MnO_2 nanocomposites, Chemical Engineering Journal 2012, April, 1, 187, 45-52, DOI: 10.1016/j.cej.2012.01.073.

[17] Verma S., Daverey A., Sharma A., Slow sand filtration for water and wastewater treatment, A review, Environmental Technology Reviews 2017, January, 1, 6(1), 47-58, DOI: 10.1080/21622515.2016.1278278.

[18] Sun Q., Wang D., Li Y., Zhang J., Ye S., Cui J., Chen L., Wang Z., Butt H.J., Vollmer D., Deng X., Surface charge printing for programmed droplet transport, Nature Materials 2019, 18(9), 936-941, DOI: 10.1016/j.cjche.2019.05.003.

[19] Zhu Y., Murali S., Cai W., Li X., Sun J.W., Potts J.R., Ruoff R.S., Graphene and graphene oxide: Synthesis, properties, and applications, Advanced Materials 2010, 22-35, DOI: 10.1002/adma.201001068.

[20] Zaaba N.I., Foo K.L., Hashim U., Tan S.J., Liu W.W., Voon C.H., Synthesis of graphene oxide using modified hummers method: Solvent influence, Procedia Engineering 2017, January, 1, 184, 469-477, DOI: 10.1016/j.proeng.2017.04.118.

[21] Cacicedo M.L., Manzo R.M., Municoy S., Bonazza H.L., Islan G.A., Desimone M., Bellino M., Mammarella E.J., Castro G.R., Immobilized enzymes and their applications, [In:] Advances in Enzyme Technology, Elsevier 2019, January, 1, 169-200.

[22] Kuilla T., Bhadra S., Yao D., Kim N.H., Bose S., Lee J.H., Recent advances in graphene based polymer composites, Progress in Polymer Science 2010, November, 1, 35(11), 1350-1375, DOI: 10.1016/j.progpolymsci.2010.07.005.

[23] Marcano D.C., Kosynkin D.V., Berlin J.M.. Sinitskii A., Sun Z., Slesarev A., Alemany L.B., Lu W., Tour J.M., Improved synthesis of graphene oxide, ACS Nano 2010, 4, 4806-4814, DOI: 10.1021/nn1006368.

[24] Gao W., Majumder M., Alemany L.B., Narayanan T.N., Ibarra M.A., Pradhan B.K., Ajayan P.M., Engineered graphite oxide materials for application in water purification, ACS Applied Materials & Interfaces 2011, June, 22, 3(6), 1821-1826, DOI: 10.1021/am200300u.

[25] Dubey R., Bajpai J., Bajpai A.K., Green synthesis of graphene sand composite (GSC) as novel adsorbent for efficient removal of Cr(VI) ions from aqueous solution, Journal of Water Process Engineering 2015, April, 1, 5, 83-94, DOI: 10.1016/j.jwpe.2015.01.004.

[26] Li Z., Wang R., Young R.J., Deng L., Yang F., Hao L., Jiao W., Liu W., Control of the functionality of graphene oxide for its application in epoxy nanocomposites, Polymer 2013, November, 1, 54(23), 6437-6446, DOI: 10.1016/j.polymer.2013.09.054.

[27] Sitko R., Turek E., Zawisza B., Malicka E., Talik E., Heimann J., Gagor A., Feist B., Wrzalik R., Adsorption of divalent metal ions from aqueous solutions using graphene oxide, Dalton Transactions 2013, 42(16), 5682-5689, DOI: 10.1039/C3DT33097D.

[28] Sun Y., Wang Q., Chen C., Tan X., Wang X., Interaction between Eu(III) and graphene oxide nanosheets investigated by batch and extended X-ray absorption fine structure spectroscopy and by modeling techniques, Environmental Science & Technology 2012, June, 5, 46(11), 6020-6027, DOI: 10.1021/es300720f.

[29] Zhao G., Wen T., Yang X., Yang S., Liao J., Hu J., Shao D., Wang X., Preconcentration of U(VI) ions on few-layered graphene oxide nanosheets from aqueous solutions, Dalton Transactions 2012, 41(20), 6182-6188, DOI: 10.1039/C2DT00054G.

[30] Ghenaatian H.R., Shakourian-Fard M., Kamath G., Adsorption mechanism of toxic heavy metal ions on oxygen-passivated nanopores in graphene nanoflakes, Journal of Materials Science 2020, November, 55, 15826-15844.

[31] Amosa M.K., Sorption of water alkalinity and hardness from high-strength wastewater on bifunctional activated carbon: process optimization, kinetics, and equilibrium studies, Environmental Technology 2016, August, 17, 37(16), 2016-2039, DOI: 10.1080/09593330.2016.1139631.

[32] Kumarasinghe A.R., Perera W.P., Bandara J., Rukshagini P., Jayarathe L., Liyanage J.A., Tennakone R., Bandara A., Xing C.H., Weerasooriya R., Multiple coated graphite oxide-sand composites for fluoride removal in water, Journal of Environmental Chemical Engineering 2021, April, 1, 9(2), 104962, DOI: 10.1016/j.jece.2020.104962.

[33] Yu H., Zhang B., Bulin C., Li R., Xing R., High-efficient synthesis of graphene oxide based on improved hummers method, Scientific Reports 2016, November, 3, 6(1), 36143, DOI: 10.1038/srep36143.

[34] Kottegoda I.R., Gao X., Nayanajith L.D., Manorathne C.H., Wang J., Wang J.Z., Liu H.K., Gofer Y., Comparison of few-layer graphene prepared from natural graphite through fast synthesis approach. Journal of Materials Science & Technology 2015, September, 1, 31(9), 907-12, DOI: 10.1016/j.jmst.2015.07.014.

[35] Patil R.A., Zodape S.P., X-ray diffraction and sem investigation of solidification/stabilization of nickel and chromium using fly ash, Journal of Chemistry 2011, December, 1, 8, S395-403, DOI: 10.1155/2011/.

[36] Johra F.T., Lee J.W., Jung W.G., Facile and safe graphene preparation on a solution-based platform, Journal of Industrial and Engineering Chemistry 2014, September, 25, 20(5), 2883-2887, DOI: 10.1016/j.jiec.2013.11.022.

[37] Wang S., Wu L., Hu X., Zhang L., O'Donnell K.M., Buckley C.E., Li C.Z., An X-ray photoelectron spectroscopic perspective for the evolution of O-containing structures in char during gasification, Fuel Processing Technology 2018, April, 1, 172, 209-215, DOI: 10.1016/j.fuproc.2017.12.019.

[38] Sadri R., Hosseini M., Kazi S.N., Bagheri S., Zubir N., Solangi K.H., Zaharinie T., Badarudin A., A bio-based, facile approach for the preparation of covalently functionalized carbon nanotubes aqueous suspensions and their potential as heat transfer fluids, Journal of Colloid and Interface Science 2017, October, 15, 504, 115-123, DOI: 10.1016/j.jcis.2017.03.051.

[39] Udawatta M.M., De Silva R.C., De Silva D.S., Surface modification of Trema orientalis wood biochar using natural coconut vinegar and its potential to remove aqueous calcium ions: column and batch studies, Environmental Engineering Research 2023, February, 28(1), DOI: 10.4491/eer.2022.617.

[40] Milella E., Cosentino F., Licciulli A., Massaro C., Preparation and characterisation of titania/hydroxyapatite composite coatings obtained by sol-gel process, Biomaterials 2001, June, 1, 22(11), 1425-1431, DOI: 10.1016/S0142-9612(00)00300-8.

[41] Grosvenor A.P., Kobe B.A., Biesinger M.C., McIntyre N.S., Investigation of multiplet splitting of Fe 2p XPS spectra and bonding in iron compounds. Surface and Interface Analysis: An International Journal Devoted to the Development and Application of Techniques for the Analysis of Surfaces, Interfaces and Thin Films 2004, December, 36(12), 1564--1574, DOI: 10.1002/sia.1984.

[42] Moughaoui F., Ouaket A., Eddebbagh M., Bennamara A., Abourriche A., Anbaoui Z., Berrada M., 7th International Conference on Innovation in Chemical, Agricultural, Biological and Environmental Sciences (ICABES) 2017, 59-65.

[43] Nethaji S., Sivasamy A., Mandal A.B., Adsorption isotherms, kinetics and mechanism for the adsorption of cationic and anionic dyes onto carbonaceous particles prepared from Juglans regia shell biomass, International Journal of Environmental Science and Technology 2013, March, 10, 231-242, DOI: 10.1007/s13762-012-0112-0.

[44] Pandey P.K., Sharma S.K., Sambi S.S., Kinetics and equilibrium study of chromium adsorption on zeolite NaX, International Journal of Environmental Science & Technology 2010, March 7, 395-404. DOI: 10.1007/BF03326149.

[45] Smith R.A., Biographical memoirs of fellows of the royal society, British Medical Journal 1976, April, 24, 1021.

[46] Afkhami A., Moosavi R., Adsorptive removal of Congo red, a carcinogenic textile dye, from aqueous solutions by maghemite nanoparticles, Journal of Hazardous Materials 2010, February, 15, 174(1-3), 398-403, DOI: 10.1016/j.jhazmat.2009.09.066.

[47] Mohan S., Kumar V., Singh D.K., Hasan S.H., Synthesis and characterization of rGO/ZrO_2 nanocomposite for enhanced removal of fluoride from water: kinetics, isotherm, and thermodynamic modeling and its adsorption mechanism, RSC Advances 2016, 6(90), 87523-38, DOI: 10.1039/C5RA20601D.

[48] Priyadarshini B., Rath P.P., Behera S.S., Panda S.R., Sahoo T.R., Parhi P.K., IOP Conference Series: Materials Science and Engineering 2018, 310, 1, 012051, IOP Publishing.

[49] Nethaji S., Sivasamy A., Mandal A.B., Adsorption isotherms, kinetics and mechanism for the adsorption of cationic and anionic dyes onto carbonaceous particles prepared from Juglans regia shell biomass, International Journal of Environmental Science and Technology 2013, March, 10, 231-242, DOI: 10.1007/s13762-012-0112-0.

[50] Sharma M., Hazra S., Basu S., Kinetic and isotherm studies on adsorption of toxic pollutants using porous ZnO@ SiO2 monolith, Journal of Colloid and Interface Science 2017, October, 15, 504, 669-679, DOI: 10.1016/j.jcis.2017.06.020.

[51] Katsumi T., Soil excavation and reclamation in civil engineering: Environmental aspects, Soil Science and Plant Nutrition 2015, July, 10, 61(sup1), 22-29, DOI: 10.1080/00380768.2015.1020506.

[52] Achmad A., Kassim J., Suan T.K., Amat R.C., Seey T.L., Equilibrium, kinetic and thermodynamic studies on the adsorption of direct dye onto a novel green adsorbent developed from Uncaria gambir extract, Journal of Physical Science 2012, 23(1), 1-3.

[53] Singh R.K., Kumar R., Singh D.P., Graphene oxide: strategies for synthesis, reduction and frontier applications, RSC Advances 2016, 6(69), 64993-65011, DOI: 10.1039/C6RA07626B.

[54] Alam S.N., Sharma N., Kumar L., Synthesis of graphene oxide (GO) by modified hummers method and its thermal reduction to obtain reduced graphene oxide (rGO), Graphene 2017, January, 10, 6(1), 1-8, DOI: 10.4236/graphene.2017.61001.

[55] Gao W., Majumder M., Alemany L.B., Narayanan T.N., Ibarra M.A., Pradhan B.K., Ajayan P.M., Engineered graphite oxide materials for application in water purification, ACS Applied Materials & Interfaces 2011, June, 22, 3(6), 1821-6, DOI: 10.1021/am200300u.

[56] Vigdorowitsch M., Pchelintsev A., Tsygankova L., Tanygina E., Freundlich isotherm: An adsorption model complete framework, Applied Sciences 2021, August, 31, 11(17), 8078, DOI: 10.3390/app11178078.

[57] Lee E.J., Lim K.H., A dynamic adsorption model for the gas-phase biofilters treating ethanol: Prediction and validation, Korean Journal of Chemical Engineering 2012, October, 29, 1373-1381, DOI: 10.1007/s11814-012-0063.

[58] Tran H.N., Applying linear forms of pseudo-second-order kinetic model for feasibly identifying errors in the initial periods of time-dependent adsorption datasets, Water 2023, March, 21, 15(6), 1231, DOI: 10.3390/w15061231.

[59] Wang M., Niu Y., Zhou J., Wen H., Zhang Z., Luo D., Gao D., Yang J., Liang D., Li Y., The dispersion and aggregation of graphene oxide in aqueous media, Nanoscale 2016, 8(30), 14587-14592, DOI: 10.1039/C6NR03503E.

[60] Jia F., Xiao X., Nashalian A., Shen S., Yang L., Han Z., Qu H., Wang T., Ye Z., Zhu Z., Huang L., Advances in graphene oxide membranes for water treatment, Nano Research 2022, July, 15(7), 6636-6654, DOI: 10.1007/s12274-022-4273-y.

[61] Møllebjerg A., Meyer R.L., Biofouling Control in Water Filtration Systems. InAntibiofilm Strategies: Current and Future Applications to Prevent, Control and Eradicate Biofilms 2022, September 29, 521-551, International Publishing, Cham, Springer, DOI: 10.1007/978-3-031-10992-8_20.

View publication stats